



Nucleation pathways on complex networks

Chuansheng Shen, Hanshuang Chen, Miaolin Ye, and Zhonghuai Hou

Citation: *Chaos: An Interdisciplinary Journal of Nonlinear Science* **23**, 013112 (2013); doi: 10.1063/1.4790832

View online: <http://dx.doi.org/10.1063/1.4790832>

View Table of Contents: <http://scitation.aip.org/content/aip/journal/chaos/23/1?ver=pdfcov>

Published by the [AIP Publishing](#)

Articles you may be interested in

[Chaotification of complex networks with impulsive control](#)

Chaos **22**, 023137 (2012); 10.1063/1.4729136

[Cascading dynamics in complex quantum networks](#)

Chaos **21**, 025107 (2011); 10.1063/1.3598453

[Announcement: Focus Issue on "Mesoscales in Complex Networks"](#)

Chaos **20**, 010202 (2010); 10.1063/1.3298887

[Synchronization-based scalability of complex clustered networks](#)

Chaos **18**, 043109 (2008); 10.1063/1.3005782

[Announcement: Focus issue on "Synchronization in complex networks"](#)

Chaos **17**, 040201 (2007); 10.1063/1.2811702

computing
IN SCIENCE & ENGINEERING

AIP's JOURNAL OF COMPUTATIONAL TOOLS AND METHODS.
AVAILABLE AT MOST LIBRARIES.

Nucleation pathways on complex networks

Chuansheng Shen,^{1,2} Hanshuang Chen,³ Miaolin Ye,² and Zhonghuai Hou^{1,a)}

¹*Hefei National Laboratory for Physical Sciences at Microscales, and Department of Chemical Physics, University of Science and Technology of China, Hefei 230026, China*

²*School of Mathematics and Computation Sciences, Anqing Normal University, Anqing 246011, China*

³*School of Physics and Material Science, Anhui University, Hefei 230039, China*

(Received 10 September 2012; accepted 15 January 2013; published online 7 February 2013)

Identifying nucleation pathway is important for understanding the kinetics of first-order phase transitions in natural systems. In the present work, we study nucleation pathway of the Ising model in homogeneous and heterogeneous networks using the forward flux sampling method, and find that the nucleation processes represent distinct features along pathways for different network topologies. For homogeneous networks, there always exists a dominant nucleating cluster to which relatively small clusters are attached gradually to form the critical nucleus. For heterogeneous ones, many small isolated nucleating clusters emerge at the early stage of the nucleation process, until suddenly they form the critical nucleus through a sharp merging process. Moreover, we also compare the nucleation pathways for different degree-mixing networks. By analyzing the properties of the nucleating clusters along the pathway, we show that the main reason behind the different routes is the heterogeneous character of the underlying networks. © 2013 American Institute of Physics. [<http://dx.doi.org/10.1063/1.4790832>]

Nucleation is essential for many dynamical processes on real-world scenarios, such as crystallization, fractures, glass formation, and protein folding. Since complex networks can model many real systems, in this contribution, therefore, we show how local patterns of nucleation emerge differently in homogeneous and heterogeneous complex networks, driving the critical nucleus come into being following different pathways. Furthermore, the effects of degree correlation on nucleation pathway are also studied. The dependence of the dynamics on the topology is unveiled. This study provides a new perspective and approach to understand many first-order phase transitions in natural and social systems.

I. INTRODUCTION

Nucleation is a fluctuation-driven process that initiates the decay of a metastable state into a more stable one.¹ It is usually involved in first-order phase transitions and along with growth of a new phase.²⁻⁴ Many important phenomena in nature, including crystallization,^{5,6} fractures,^{7,8} glass formation,⁹ and protein folding,¹⁰ to list just a few, are associated with nucleation. Despite much attention, many aspects of nucleation processes in complex systems are still unclear and deserve more investigation.

The Ising model is a paradigm for many phenomena in statistical physics. It has also been widely used to study the nucleation process. For instance, in two-dimensional lattices, Allen *et al.* discovered that shear can enhance the nucleation rate and the rate peaks at an intermediate shear rate.¹¹ Sear found that a single impurity may considerably enhance the nucleation rate.¹² Page and Sear reported that the existence

of a pore may lead to two-stage nucleation, and the overall nucleation rate can reach a maximum level at an intermediate pore size.¹³ The nucleation pathway of the Ising model in three-dimensional lattices has also been studied by Sear and Pan.^{14,15} In addition, the Ising model has been frequently used to test the validity of classical nucleation theory (CNT).¹⁶⁻²² Nevertheless, all these studies are limited to regular lattices in Euclidean space.

Since many real systems can be properly modeled by network-organized structure,²³⁻²⁵ it is thus an interesting topic to explore nucleation process in complex networks. Very recently, our group has studied nucleation dynamics on scale-free (SF) networks²⁶ and modular networks.²⁷ In these two papers, we mainly focused on the nucleation rate and system size effects. We found that, for SF networks, the nucleation rate decays exponentially with network size, while the critical nucleus size increases linearly. For modular networks, as the network modularity worsens the nucleation undergoes a transition from a two-step to one-step process and the nucleation rate shows a nonmonotonic dependence on the modularity. As we know, network topology could play an important role in the system's dynamics, involving not only the stationary properties but also the dynamical pathways. For example, it was shown that network heterogeneity could drastically influence the path to oscillator synchronization.²⁸ Nevertheless, how network topology would influence the nucleation pathway is still an open question. Motivated by this, we will study the different roles of network architectures in the formation of nucleating clusters, which can reveal the nucleation pathways of the Ising model in the underlying networks.

Since nucleation is an activated process, it can be extremely slow. Therefore, direct simulations can take excessive amounts of time. To overcome this difficulty, in the present work, we adopt the forward flux sampling (FFS)²⁹

^{a)}Electronic address: hzhlj@ustc.edu.cn.

approach proposed recently, which is efficient and easy to implement to study rare events. We employ Erdős-Rényi (ER) and SF networks as the paradigm of homogeneous and heterogeneous networks respectively. By using FFS, we obtain lots of configurations at each interface along the nucleation pathway. From these configurations we scrutinize and compare the nucleating clusters in ER and SF networks. It is found that the processes of forming the critical nucleus are qualitatively different between the two cases of networks. For the former, a dominant cluster arise first, and groups smaller clusters gradually, while for the latter, many small clusters emerge at first and then abruptly turn into the critical nucleus. Interestingly, both the cluster size distributions follow power-law distributions and the slopes are nearly the same at early nucleation stage.

The paper is organized as follows. Section II presents the details of our simulation model and the numerical methods we employ to sampling the nucleation pathway. In Sec. III, the numerical results are compared for SF networks and ER ones, as well as for different degree-mixing networks. A brief summary and discussion are given in Sec. IV.

II. MODEL AND METHOD

A. Network-organized Ising model

We consider the Ising model on complex networks consisting of N nodes. Note that there exists a number of simulations and analytical results for the Ising model in ER and SF networks.^{30–32} Each node is endowed with a spin variable s_i that can be either $+1$ (up) or -1 (down). The Hamiltonian of the system is given by

$$H = -J \sum_{i < j} A_{ij} s_i s_j - h \sum_i s_i, \quad (1)$$

where J is the coupling constant and h is the external magnetic field. For convenience, we set $J = 1$ in the following discussions. The elements of the adjacency matrix of the network take $A_{ij} = 1$ if nodes i and j are connected and $A_{ij} = 0$ otherwise. The degree, that is the number of neighboring nodes, of node i is defined as $k_i = \sum_{j=1}^N A_{ij}$.

The system evolves in time according to single-spin-flip dynamics with Metropolis acceptance probabilities,³³ in which we attempt to flip each spin once, on average, during each Monte Carlo (MC) cycle. In each attempt, a randomly chosen spin is flipped with the probability $\min(1, e^{-\beta\Delta E})$, where $\beta = 1/(k_B T)$ with k_B being the Boltzmann constant and T is the temperature, and ΔE is the energy change due to the flipping process. In the absence of an external magnetic field, the system undergoes an order-disorder phase transition at the critical temperature. Above the critical temperature, the system is disordered where up- and down-pointing spins are roughly equally abundant. Below the critical temperature, the system prefers to be in either of the two states: one state with predominantly up spins, and the other with almost down spins. In the presence of a small external field, one of these two states becomes metastable, and if initiated predominantly in this metastable state, the system will remain for a significantly long time before it undergoes a

nucleation transition to the thermodynamically stable state. We are interested in the pathways for this transition.

B. FFS method

The FFS method has been successfully used to calculate rate constants and transition paths for rare events in equilibrium and nonequilibrium systems.^{11–13,29,34,35} For clarity, we describe the method again here, together with some relevant details with our work. This method uses a series of interfaces in phase space between the initial and final states to force the system from the initial state A to the final state B in a ratchet-like manner. Before the simulation begins, an reaction coordinate λ is first defined, such that the system is in state A if $\lambda < \lambda_0$ and it is in state B if $\lambda > \lambda_M$. A series of nonintersecting interfaces λ_i ($0 < i < M$) lie between states A and B , such that any path from A to B must cross each interface without reaching λ_{i+1} before λ_i . The algorithm first runs a long-time simulation which gives an estimate of the flux escaping from the basin of A and generates a collection of configurations corresponding to crossings of interface λ_0 . The next step is to choose a configuration from this collection at random and use it to initiate a trial run which is continued until it either reaches λ_1 or returns to λ_0 . If λ_1 is reached, the configuration of the end point of the trial run is stored. This process is repeated, step by step, until λ_M is reached. For more detailed descriptions of the FFS method please see Ref. 36.

In this work, we will use FFS to study nucleation pathways of the equilibrium phase from the metastable spin phase. Specifically, we let $h > 0$ and start from an initial state with $s_i = -1$ for most of the spins. We define the order parameter λ as the total number of up spins in the network. The spacing between adjacent interfaces is fixed at 3 up spins. We perform 1000 trials per interface for each FFS sampling, from which at least 200 configurations are saved in order to investigate the statistical properties along the nucleation pathway. The results are obtained by averaging over 10 independent FFS samplings and 50 different network realizations.

III. NUMERICAL RESULTS

A. Uncorrelated networks

In what follows, we employ a Barabási-Albert (BA) SF network, whose degree distribution follows a power law $P(k) \sim k^{-\gamma}$ with the scaling exponent $\gamma = 3$,³⁷ and the well-known ER random network.³⁸

In Figure 1, we present schematically the evolution of local nucleating clusters in ER and SF networks at different stages (for clarity only show 100 nodes). Here, a nucleating cluster is defined as the component of connected nodes with up spins. Qualitatively, it shows distinct features along nucleation stages. In the ER case, there always exists a dominant cluster, which groups smaller ones gradually. While for SF networks, no dominant cluster appears at the early stage, but then a giant cluster emerges suddenly. This demonstrates that nucleation follows different pathways on ER and SF

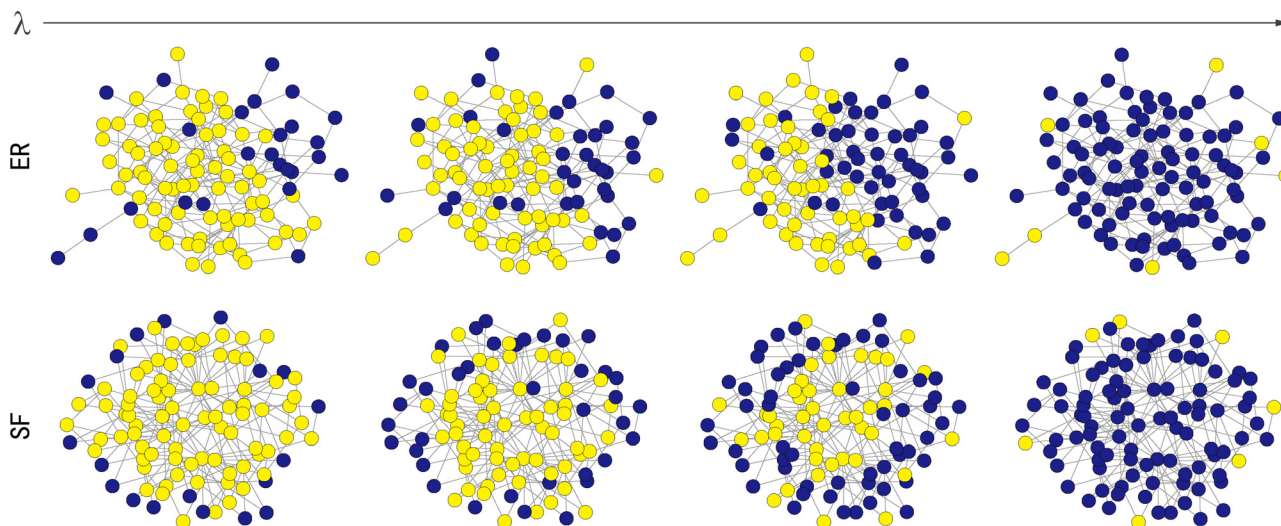


FIG. 1. Typical nucleating clusters for several values of λ for the two different topologies studied (ER and SF). These shown networks contain 100 nodes and 4 mean degree, in order to have a sizeable picture of the system. Up spins and down spins are indicated by blue and yellow circles, respectively.

networks, indicating that heterogeneity of the network topology may play an important role.

To further elucidate detailed characteristics along the nucleation pathway, we use FFS to generate configurations and perform detailed analysis on the nucleating clusters, including the largest cluster size, average degree of the cluster nodes, the number of clusters and cluster size distribution. According to CNT, there exists a critical nucleus size λ_c of the new phase, above which the system grows rapidly to the new phase. Herein, we mainly focus on the nucleation stage where $\lambda < \lambda_c$. In our simulation, we determine λ_c by computation of the committor probability P_B , which is the probability of reaching the thermodynamic stable state before returning to the metastable state. As commonly reported in the literature,^{15,21} the critical nucleus appears at $P_B(\lambda_c) = 0.5$. Since λ_c are different for different networks, we thus introduce λ/λ_c as the control parameter.

For consistent comparison, we introduce S_{\max} as the ratio of the size of the largest nucleating cluster to the total number of up spins, and plot S_{\max} (averaged over the ensemble at each interface) as a function of λ/λ_c in Figure 2.

Clearly, one can see that S_{\max} for ER networks is always larger than that for SF ones. Specifically, at $\lambda/\lambda_c = 0.5$, S_{\max} is already more than 70% for ER networks, while it is only about 30% for SF ones, as shown by the dashed gray lines in Figure 2. But when $\lambda/\lambda_c = 1$ they almost tend to 100% together.

To show our results more explicitly, we investigate the average degree K_n of the nodes inside the nucleating clusters, and plot K_n as a function of λ/λ_c in Figure 3. As shown, K_n increases monotonically with λ/λ_c for both ER and SF networks, which means the new phase tends to grow from those nodes with smaller degrees. For ER networks, K_n grows fast at the very beginning following by a relatively slow increasing. For SF networks, K_n increases slowly at first and jumps sharply when approaching the critical nucleus. Such a scenario is consistent with Figures 1 and 2.

To better understand the aforementioned differences, we present the number N_s of the nucleating clusters as a function of λ/λ_c in Figure 4(a). We observe that N_s non-monotonically depends on λ/λ_c and the numbers of clusters in SF networks are always more than that in ER ones. On the

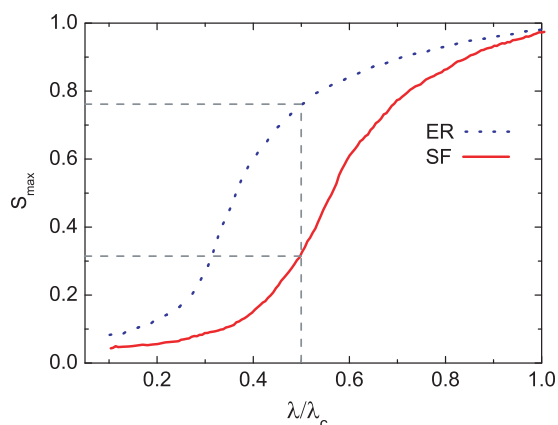


FIG. 2. The relative size S_{\max} of the largest cluster as a function of λ/λ_c . Parameters are $N=1000$, the average network degree $K=6$, $h=0.5$, $T/T_c = 0.3$, $\lambda_0 = 130$, and $\lambda_M = 880$.

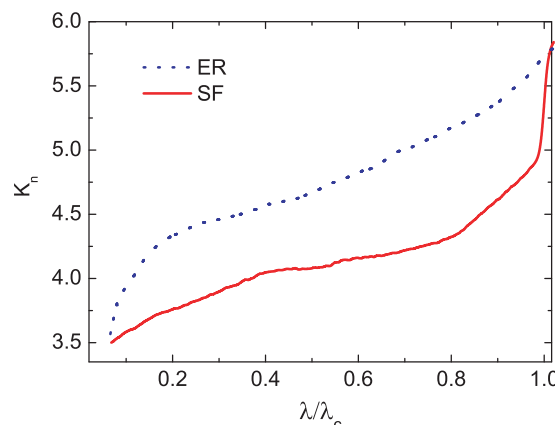


FIG. 3. Average degree K_n of new phase nodes as a function of λ/λ_c . Other parameters are the same as in Fig. 2.

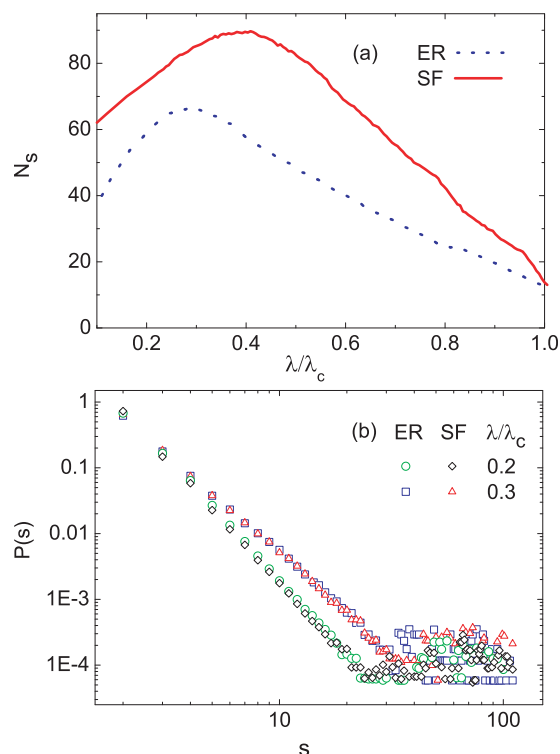


FIG. 4. (a) The number N_s of nucleating clusters as a function of λ/λ_c . (b) Size distribution $P(s)$ of nucleating clusters, on a log-log scale, s denote the size of nucleating clusters. Other parameters are the same as in Fig. 2.

other hand, N_s for both networks approach the same magnitude near the formation of critical nucleus, but it decreases much more sharply in SF networks which is also consistent with the picture shown in Figures 1 to 3. In Figure 4(b), the cluster size distributions $P(s)$ for $\lambda/\lambda_c = 0.2$ and 0.3 are shown. Interestingly, $P(s)$ follow apparent power-law distributions in the small size range for both types of networks, and in addition, the exponents are nearly equivalent for the same λ/λ_c . The power law breaks in the large size range, where large clusters dominate.

The above results can be qualitatively understood in terms of CNT. CNT assumes that the formation of a nucleus lies in two competing factors: the bulk energy gain of creating a new up spin which favors the growth of the nucleus, and the interfacial energy cost, an opposing factor, which is due to the creation of new boundary links between up and down spins. That is, the change of free energy ΔF may be written as $\Delta F(\lambda) = -2h\lambda + \sigma\lambda$, where σ denotes the effective interfacial free energy, which mainly depends on the average number of boundary links that an up-spin node has. Obviously, a node with more boundary links is more difficult to change its spin state. For SF networks, it is thus always easier for the leaf nodes with small degrees to change state than the hubs with large degrees. Since the degree distribution follows power-law, there exist a lot of hubs with intermediate degrees, as well as a few hubs with very large degrees. Usually, many leaf nodes are connected to relatively small hubs, which are further connected to large hubs. Therefore, only small nucleating clusters, consisted of leaf nodes and small hubs, can form at the early stage of the nucleation process. These small clusters are either away from each other

on the network or separated by those crucial hubs with very large degrees. In the final stage of the nucleation, once the crucial hubs connecting these small clusters change their states, a giant nucleation cluster will emerge abruptly. This picture is consistent with those results shown in the above figures. For ER networks, however, the degree distribution follows Poisson distribution and no crucial hub exists, such that those new-formed clusters are usually connected together and one would not expect a sharp increase in the cluster size, which is observed in SF networks.

B. Degree correlated networks

It is worthy noting that the above numerical demonstrations are carried out on degree uncorrelated networks. As we know, in real-world networks, degree correlation is an ubiquitous feature. For instance, social networks show that nodes with large degrees tend to connect together, a property referred to as “assortative mixing”.³⁹ In contrast, many technological and biological networks show “disassortative mixing,” i.e., connections between high-degree and low-degree nodes are more probable.^{40,41} Previous studies showed that correlations may play important roles in network dynamics.^{39–43} To measure the degree of the correlation, in Ref. 39 Newman introduced a degree-mixing coefficient

$$r = \frac{m^{-1} \sum_i j_i k_i - \left[m^{-1} \sum_i (j_i + k_i) / 2 \right]^2}{m^{-1} \sum_i (j_i^2 + k_i^2) / 2 - \left[m^{-1} \sum_i (j_i + k_i) / 2 \right]^2}. \quad (2)$$

Here m is the total number of edges in the network, j_i and k_i are the degrees of the two end-nodes of the i -th edge. r is zero for networks with no degree-correlation, such as BA-SF networks, and positive or negative for assortative or disassortative mixing networks, respectively.

In the following, we will show that the effects of degree-degree correlation on the nucleation pathways. We first generate a regular SF network by using the BA model³⁷ with power-law degree distribution $P(k) \sim k^{-3}$. Then using the algorithm as proposed in Ref. 39, we convert this uncorrelated SF network into a correlated one.

Figure 5 displays the relative S_{\max} , K_n , N_s , and the average size of nucleating cluster $\langle S \rangle$ as a function of λ/λ_c for three different degree-mixing networks. It is shown that, the four quantities exhibit different behaviors for different degree-mixing cases. First, S_{\max} in assortative mixing network grows faster than the others in the early nucleation stage, and then it increases slower, as shown in Figure 5(a). Second, the jump of K_n in assortative network is sharper than that in uncorrelated network at the critical nucleus forming, while for disassortative network it becomes gradually, as shown in Figure 5(b). Third, N_s in disassortative mixing network is the largest (shown by the solid blue line in Figure 5(c)) but in assortative one the smallest. Lastly, $\langle S \rangle$ in assortative network is much larger than that in the others, especially, it is smallest for disassortative network. As mentioned above, nucleation always starts from nodes with smaller degree, and nodes with higher degree are more stable. Therefore, the high-degree nodes in a assortative network, which

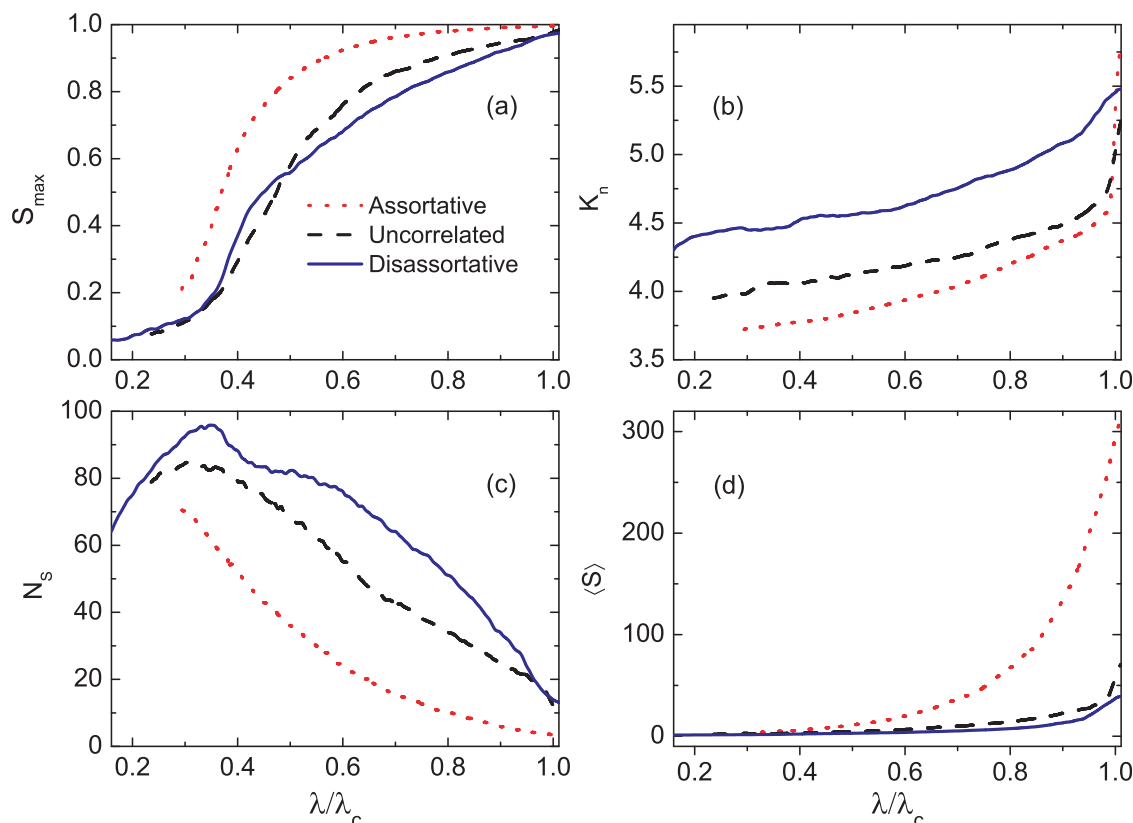


FIG. 5. The relative S_{\max} , K_n , N_s , and $\langle S \rangle$ as a function of λ/λ_c for assortative, uncorrelated, and disassortative degreemixing networks, corresponding to $r = 0.2, 0, -0.2$, respectively. Other parameters are the same as in Fig. 2.

preferring to connect together, always hard to flip. Once these connected hubs flip together, the nucleating cluster increases explosively, which is shown by the steep jump in Figures 5(b) and 5(d). While for disassortative networks, wherein the low-degree nodes separate the high-degree nodes, the hubs does not flip simultaneously, so the nucleating cluster grows gradually.

IV. DISCUSSION AND CONCLUSIONS

The nucleation phenomenon is closely related to the front propagation in bistable reaction-diffusion systems. In a very recent paper,⁴⁴ Kouvaris *et al.* have studied the traveling and stationary patterns in bistable one-component systems placing on various networks. They showed nodes with small degrees favor the fronts propagation and the fronts propagate smoothly in the ER (homogeneous) networks, whereas in the SF (heterogeneous) networks the fronts first propagate to nodes with small degrees and when a critical number of such nodes is activated, the front spreads rapidly in the rest of the system. This rapid change in the SF networks seems to share similarities with the present results of nucleation in the Ising model. However, Barthélemy *et al.*⁴⁵ revealed a different mechanism about the propagation of infections in heterogeneous networks. The infection first affects the hubs and next it invades rapidly the other nodes, affecting progressively the nodes with decreasing degrees. This means that nodes with smaller degrees will change their state to infected later. This mechanism seems to be opposite to the present one in this paper, but the rapid behavior still exists in the SF networks. Furthermore,

we should note that in our previous work, we mainly investigated the effect of network size on nucleation size and the size of critical nucleus. While in the present study, we focus on the identification of the pathway of nucleating clusters on diverse networks that is equally important aspect of nucleation phenomenon.

In summary, we have studied nucleation pathways of the Ising model with Metropolis spin-flip dynamics in ER and SF networks using the FFS method. Concerning the former, there always exists a dominant cluster which groups small clusters gradually until the critical nucleus is formed; while concerning the latter, many isolated small clusters grow separately which suddenly merge together into the critical nucleus. We have performed detailed analysis involving the nucleating clusters along the nucleation pathway, including the cluster size as well as its distribution, the mean degree inside the cluster, and so on, to further demonstrate the above scenario. In addition, the nucleation pathways for different degree-mixing networks are also compared. The distinct nucleation pathways further emphasize the very important role of network topology. Our study may provide a better understanding of how first-order phase transitions take place on complex networks, which could be of great importance not only for physical systems but also for social and biological networks.

ACKNOWLEDGMENTS

This work was supported by the National Natural Science Foundation of China (Grants Nos. 21125313, 20933006, 91027012, and 11205002). C.S.S. was also

supported by the Key Scientific Research Fund of Anhui Provincial Education Department (Grant No. KJ2012A189).

- ¹D. Kashchiev, *Nucleation: Basic Theory With Applications* (Butterworths-Heinemann, Oxford, 2000).
- ²P. Hänggi, P. Talkner, and M. Borkovec, *Rev. Mod. Phys.* **62**, 251 (1990).
- ³A. Laaksonen, V. Talanquer, and D. W. Oxtoby, *Annu. Rev. Phys. Chem.* **46**, 489 (1995).
- ⁴V. J. Anderson and H. N. Lekkerkerker, *Nature (London)* **416**, 811 (2002).
- ⁵L. Gránásy and F. Igloi, *J. Chem. Phys.* **107**, 3634 (1997).
- ⁶P. Asanithi, E. Saridakis, L. Govada, I. Jurewicz, E. W. Brunner, R. Ponnusamy, J. A. S. Cleaver, A. B. Dalton, N. E. Chayen, and R. P. Sear, *ACS Appl. Mater. Interfaces* **1**, 1203 (2009).
- ⁷D. A. Lockner, J. D. Byerlee, V. Kukusenko, A. Ponomarev, and A. Sidorin, *Nature (London)* **350**, 39 (1991).
- ⁸A. Garchimartin, A. Guarino, L. Bellon, and S. Ciliberto, *Phys. Rev. Lett.* **79**, 3202 (1997).
- ⁹G. Johnson, A. I. Mel'čuk, H. Gould, W. Klein, and R. D. Mountain, *Phys. Rev. E* **57**, 5707 (1998).
- ¹⁰A. R. Fersht, *Proc. Natl. Acad. Sci. U.S.A.* **92**, 10869 (1995).
- ¹¹R. J. Allen, C. Valeriani, S. Tanase-Nicola, P. R. ten Wolde, and D. Frenke, *J. Chem. Phys.* **129**, 134704 (2008).
- ¹²R. P. Sear, *J. Phys. Chem. B* **110**, 4985 (2006).
- ¹³A. J. Page and R. P. Sear, *Phys. Rev. Lett.* **97**, 065701 (2006).
- ¹⁴R. P. Sear, *J. Chem. Phys.* **129**, 164510 (2008).
- ¹⁵A. C. Pan and D. Chandler, *J. Phys. Chem. B* **108**, 19681 (2004).
- ¹⁶M. Acharyya and D. Stauffer, *Eur. Phys. J. B* **5**, 571 (1998).
- ¹⁷V. A. Shneidman, K. A. Jackson, and K. M. Beatty, *J. Chem. Phys.* **111**, 6932 (1999).
- ¹⁸S. Wonzak, R. Strey, and D. Stauffer, *J. Chem. Phys.* **113**, 1976 (2000).
- ¹⁹K. Brendel, G. T. Barkema, and H. van Beijeren, *Phys. Rev. E* **71**, 031601 (2005).
- ²⁰D. Winter, P. Virnau, and K. Binder, *Phys. Rev. Lett.* **103**, 225703 (2009).
- ²¹S. Ryu and W. Cai, *Phys. Rev. E* **81**, 030601(R) (2010).
- ²²S. Ryu and W. Cai, *Phys. Rev. E* **82**, 011603 (2010).
- ²³R. Albert and A.-L. Barabási, *Rev. Mod. Phys.* **74**, 47 (2002).
- ²⁴S. N. Dorogovtsev and J. F. F. Mendes, *Adv. Phys.* **51**, 1079 (2002).
- ²⁵M. E. J. Newman, *SIAM Rev.* **45**, 167 (2003).
- ²⁶H. Chen, C. Shen, Z. Hou, and H. Xin, *Phys. Rev. E* **83**, 031110 (2011).
- ²⁷H. Chen and Z. Hou, *Phys. Rev. E* **83**, 046124 (2011).
- ²⁸J. Gómez-Gardeñes, Y. Moreno, and A. Arenas, *Phys. Rev. Lett.* **98**, 034101 (2007).
- ²⁹R. J. Allen, P. B. Warren, and P. R. ten Wolde, *Phys. Rev. Lett.* **94**, 018104 (2005).
- ³⁰S. N. Dorogovtsev, A. V. Goltsev, and J. F. F. Mendes, *Phys. Rev. E* **66**, 016104 (2002).
- ³¹C. P. Herrero, *Phys. Rev. E* **69**, 067109 (2004).
- ³²S. H. Lee, M. Ha, H. Jeong, J. D. Noh, and H. Park, *Phys. Rev. E* **80**, 051127 (2009).
- ³³D. P. Landau and K. Binder, *A Guide to Monte Carlo Simulations in Statistical Physics* (Cambridge University Press, Cambridge, 2000).
- ³⁴C. Valeriani, R. J. Allen, M. J. Morelli, D. Frenkel, and P. R. ten Wolde, *J. Chem. Phys.* **127**, 114109 (2007).
- ³⁵R. J. Allen, D. Frenkel, and P. R. ten Wolde, *J. Chem. Phys.* **124**, 024102 (2006).
- ³⁶R. J. Allen, C. Valeriani, and P. R. ten Wolde, *J. Phys.: Condens. Matter* **21**, 463102 (2009).
- ³⁷A.-L. Barabási and R. Albert, *Science* **286**, 509 (1999).
- ³⁸M. Molloy and B. Reed, *Random Struct. Algorithms* **6**, 161 (1995).
- ³⁹M. E. J. Newman, *Phys. Rev. Lett.* **89**, 208701 (2002).
- ⁴⁰R. Pastor-Satorras, A. Vázquez, and A. Vespignani, *Phys. Rev. Lett.* **87**, 258701 (2001).
- ⁴¹S. Maslov and K. Sneppen, *Science* **296**, 910 (2002).
- ⁴²M. Boguñá and R. Pastor-Satorras, *Phys. Rev. E* **66**, 047104 (2002).
- ⁴³J. Berg and M. Lässig, *Phys. Rev. Lett.* **89**, 228701 (2002).
- ⁴⁴N. E. Kouvaris, H. Kori, and A. S. Mikhailov, *PLoS ONE* **7**, e45029 (2012).
- ⁴⁵M. Barthélemy, A. Barrat, R. Pastor-Satorras, and A. Vespignani, *Phys. Rev. Lett.* **92**, 178701 (2004).